Relative Contribution of Greenhouse Gases and Ozone-Depleting Substances to Temperature Trends in the Stratosphere: A Chemistry–Climate Model Study

RICHARD S. STOLARSKI, ANNE R. DOUGLASS, AND PAUL A. NEWMAN

Atmospheric Chemistry and Dynamics Branch, NASA Goddard Space Flight Center, Greenbelt, Maryland

STEVEN PAWSON

Global Modeling and Assimilation Office, NASA Goddard Space Flight Center, Greenbelt, Maryland

MARK R. SCHOEBERL

Earth Sciences Division, NASA Goddard Space Flight Center, Greenbelt, Maryland

(Manuscript received 2 December 2008, in final form 29 July 2009)

ABSTRACT

The temperature of the stratosphere has decreased over the past several decades. Two causes contribute to that decrease: well-mixed greenhouse gases (GHGs) and ozone-depleting substances (ODSs). This paper addresses the attribution of temperature decreases to these two causes and the implications of that attribution for the future evolution of stratospheric temperature. Time series analysis is applied to simulations of the Goddard Earth Observing System Chemistry–Climate Model (GEOS CCM) to separate the contributions of GHGs from those of ODSs based on their different time-dependent signatures. The analysis indicates that about 60%–70% of the temperature decrease of the past two decades in the upper stratosphere near 1 hPa and in the lower midlatitude stratosphere near 50 hPa resulted from changes attributable to ODSs, primarily through their impact on ozone. As ozone recovers over the next several decades, the temperature should continue to decrease in the middle and upper stratosphere because of GHG increases. The time series of observed temperature in the upper stratosphere is approaching the length needed to separate the effects of ozone-depleting substances from those of greenhouse gases using temperature time series data.

1. Introduction

The recent United Nations Environment Programme–World Meteorological Organization (UNEP–WMO) ozone assessment report (Baldwin et al. 2007, Chap 5) states, for the lower stratosphere, ''model calculations suggest that the observed ozone loss is the predominant cause of the cooling observed over this period [1979–2005].'' It further states ''model calculations suggest that the upper-stratospheric trends are due, roughly equally, to decreases in ozone and increases in CO_2.'' These conclusions are based mainly on the results reported in Shine et al. (2003) and Langematz et al. (2003). The assessment report further states that there may be a less certain contribution to stratospheric cooling from changes in stratospheric water vapor. Over the next two decades, ozone recovery should begin to occur while greenhouse gases (GHGs) continue to increase. These two trends will have opposite effects on the temperature of the stratosphere. Additionally, because ozone chemistry depends on both temperature and the abundance of ozone-depleting substances (ODSs), Shepherd and Jonsson (2008) have pointed out the importance of distinguishing between the impact of changes in ozone versus changes in ODS on stratospheric temperature trends. In this paper we address the question of the relative importance of GHGs and ODSs on stratospheric temperatures of the recent past and the future (1960–2100).

Model sensitivity studies are commonly used to separate the effects of ozone from those of greenhouse gases. A model simulation with fixed ozone and changing greenhouse gases can be compared with a simulation with fixed greenhouse gases and changing ozone to

Corresponding author address: Richard S. Stolarski, Mail Code 613.3, NASA Goddard Space Flight Center, 8800 Greenbelt Road, Greenbelt, MD 20771.
E-mail: richard.s.stolarski@nasa.gov

DOI: 10.1175/2009JCLI2955.1

determine the individual sensitivities (Shine et al. 2003). These sensitivity studies give us a good guide for what to expect from each source of perturbation. The spatial fingerprints derived from sensitivity studies have been used to help identify causes for climate change (e.g., Santer et al. 2003). We adapt this concept to use time signatures, and time series analysis, to separate the effects of GHGs and ODSs on temperature in the stratosphere. The analysis will provide insight into the relative magnitudes of the effects and whether the reduction of ozone-depleting substances and recovery of ozone will lead to an increase in stratospheric temperature over next few decades or the temperature trend will be dominated by continued greenhouse gas cooling.

Greenhouse gas effects on stratospheric temperature are expected to have a signature that follows the time-dependent changes of the concentrations of GHGs such as CO_2 and CH_4. Temperature decreases in the upper stratosphere will lead to increases in ozone that reduce the cooling effect of the GHGs. We will refer to this term throughout the paper as the greenhouse gas term, or separately as the CO_2 term and the CH_4 term. The signature of temperature changes due to ODSs is expected to track equivalent effective stratospheric chlorine (EESC) [total inorganic chlorine plus 50 times total inorganic bromine, see, e.g., Newman et al. (2007)]. The primary effect of ODSs on stratospheric temperature occurs indirectly through their impact on ozone. Ozone losses, caused by catalytic reactions of chlorine and bromine compounds, change the radiative heating of the stratosphere. The direct radiative effect of CFC molecules adds an increment to the temperature change that will follow the EESC time dependence. Throughout the paper we will refer to the EESC or ODS term that includes both the impacts that occur directly through ozone change and the direct radiative impacts of the ODSs. We will analyze results from 140-yr simulations with our chemistry–climate model to deduce the relative contributions of the GHG term and the ODS term to temperature change in the stratosphere. Section 2 contains a description of the chemistry–climate model along with a description of the past and future simulations. Section 2 further shows how the past and future simulations were combined into continuous time series.

Section 3 describes the time series analysis and shows results for four locations: 1) the upper stratosphere, 2) the lower midlatitude stratosphere, 3) the Antarctic lower stratosphere, and 4) the Antarctic midstratosphere. Each location illustrates important issues of past and expected future temperature change. The section includes maps of temperature sensitivity to GHG change and ODS change for the entire stratosphere. Section 4 compares the results obtained in this study to data and to published results from other models. Section 5 considers the record length necessary to obtain significant separation of the signals. Section 6 summarizes the results and discusses the implications for separating greenhouse gas effects on temperature from ozone effects on temperature in atmospheric data.

2. Description of the model and simulations

a. Model description

We use the Goddard Earth Observing System Chemistry–Climate Model (GEOS CCM) for all simulations. The GEOS CCM couples an atmospheric GCM with a stratospheric chemistry and transport model. Version 1 of the GEOS CCM is described by Pawson et al. (2008). The photochemical scheme in the model, an updated version of that used in the Goddard Chemistry and Transport Model (CTM) (e.g., Douglass and Kawa 1999), uses family approximations and has been extensively tested through applications (e.g., Douglass et al. 1989; Stolarski et al. 2006b). The CCM couples the simulated fields of O_3, CH_4, N_2O, H_2O, $CFCl_3$, and CF_2Cl_2 into its radiative code (Kiehl et al. 1998) to determine heating and cooling. The GEOS CCM was used for simulations describing a summertime increase in ozone in the Antarctic middle and upper stratosphere (Stolarski et al. 2006b). Links between the stratosphere and troposphere in the Antarctic have been examined by showing that the growth and decay of the ozone hole has a stronger impact than GHG changes on the Southern Hemisphere summertime climate change. Changes in stratospheric moisture have been examined by Oman et al. (2008), who separated the contribution of methane oxidation change from that of tropopause temperature change. Eyring et al. (2006, 2007) have compared simulations using the GEOS CCM to simulations using many other CCMs, showing a generally favorable performance in a number of aspects of the circulation. This is quantified by a model-grading exercise that reveals the GEOS CCM to be one of the better-performing models (Waugh and Eyring 2008). The GEOS CCM simulations yielded good results for the age of air in the lower stratosphere. The relationship between the mean age of air and the fractional release of chlorine from CFCs in the lower stratosphere follows the relationship derived from data (Schauffler et al. 2003; Douglass et al. 2008). These and other comparisons with observations detailed in the above references are all indications that the basic circulation produced in the model realistically represents that of the stratosphere. The main deficiencies in the simulations revealed by comparisons with observations are a high bias in total column ozone at high latitudes,

especially at times when there is no strong ozone depletion, and a late (2–3 weeks) breakup of the Antarctic vortex (Pawson et al. 2008).

b. Simulations

The objective of our simulations was to produce a continuous time series running from 1960 through the end of the twenty-first century. Sea surface temperatures (SSTs) and sea ice concentrations are specified in GEOS CCM. For the past (1960–2005) the observation-based Hadley Centre Sea Ice and Sea Surface Temperature (HadISST) dataset was used (Rayner et al. 2003). For the future (2000–99) we use SSTs generated from the Fourth Assessment Report (AR4) twenty-first-century climate simulations of two different coupled ocean–atmosphere models: the Hadley Centre Global Environmental Model version 1 (HadGEM1) (Johns et al. 2006) and National Center for Atmospheric Research (NCAR) Community Climate System Model, version 3 (CCSM3) (Collins et al. 2006). Additionally, some simulated SSTs from the same models were used for 1970–2000.

In total six simulations of GEOS CCM were used in the analysis. All simulations used specified mixing ratio boundary conditions for ODSs from the Ab scenario of WMO–UNEP (WMO 2003) and mixing ratio boundary conditions for the GHGs from the A1b scenario of the Intergovernmental Panel on Climate Change (IPCC) (Nakicenovic and Swart 2000). Two of these were past simulations starting in 1950 and extending through 2004 (labeled P1 and P2). Four "future" simulations started either in the early 1970s or late 1990s and ended near 2050 or in 2099 (labeled F1, F2, F3, and F4). (The time period for each simulation and the SSTs used are listed in Table A1. The appendix gives details of these simulations and how we constructed temperature time series that extend from 1960 through 2100. Offsets in temperature between past and future simulations occurred because of differing SSTs. These were adjusted to make continuous time series of atmospheric temperature, as described in the appendix.

3. Time series analysis of model temperature simulations

We use time series analysis to analyze the 140-yr simulated temperature records described in section 2. We assume that a temperature time series from the model simulations can be fit by a linear function of the form

$$T(t) = a_0 + a_1\mathrm{EESC}(t) + a_2\mathrm{CO_2}(t) + a_3\mathrm{CH_4}(t),$$

where $T(t)$ is temperature time series to be fit, EESC(t) is the concentration of effective stratospheric chlorine in ppbv, $CO_2(t)$ is the carbon dioxide concentration in ppmv, and $CH_4(t)$ is the methane concentration in ppmv. The coefficients a_0, a_1, a_2, and a_3 are determined by a least squares regression to the output of the model simulation and represent the mean (a_0), the sensitivity to EESC (a_1), the sensitivity to CO_2 (a_2), and the sensitivity to CH_4 (a_3). We do not consider N_2O in this paper as its time signature is a monotonic increase that will not be separable from that of CO_2. The expected small effect of N_2O on temperature will be captured by the CO_2 term in our analyses.

The EESC term used in the regression is the model global average of $Cl_y + 60Br_y$ at 1-hPa pressure, thus the EESC term captures the impact of chlorine and bromine-induced ozone change on temperature. This term will also capture the infrared radiative impact of the CFCs, a term that should be proportional to total chlorine, which is a similar time series to EESC with a relatively unimportant 4–5-yr phase shift. The CO_2 term is the largest greenhouse gas term and includes the feedback due to the ozone increase that results from decreased loss due to local cooling. The CH_4 term captures changes due to the direct radiative forcing of methane and also indirect radiative forcing of the water vapor generated by methane oxidation. It also includes any effects of changing HO_x due to changing water vapor coming from methane oxidation in the stratosphere.

In the results that follow, we use one of the 140-yr time series constructed from our combined simulations (described as P1 + F1 in the appendix). We apply statistical time series analysis to this time series to obtain the best values for the sensitivity coefficients. We compare the contributions of the different terms in units of temperature change per part per billion of the compound (EESC, CO_2, or CH_4). We use these sensitivity coefficients to calculate the temperature change due to each term over two fixed time periods: 1) the recent past (1979–98) when ozone was linearly decreasing and 2) the near future (2006–25) when ozone-depleting substances will decrease and ozone will recover and at the same time greenhouse gases are expected to continue to increase. The appendix compares results obtained from this time series to those obtained from the other ensemble members constructed from our simulations.

a. Upper stratosphere: Latitude = 40°N, pressure = 1 hPa

Temperature and ozone changes in the upper stratosphere are coupled together in a joint radiative–photochemical equilibrium (Blake and Lindzen 1973). Greenhouse gases, such as CO_2, cool the upper stratosphere by increasing infrared radiation to space. The cooler temperatures lead to an increase in ozone concentration through the slowing of temperature-dependent photochemical catalytic loss reactions. The increase in ozone concentration increases ultraviolet radiative heating,

yielding an increase in temperature that reduces the added cooling due to the CO_2 increase—a negative feedback. Thus, the upper stratosphere in 2100, after removal of most of the chlorine and bromine from CFCs and halons, will be cooler and have more ozone than the upper stratosphere of 1960 (see, e.g., Haigh and Pyle 1979, 1982; Rosenfield et al. 2002; Li et al. 2009).

Between 1960 and 2100 the chlorine and bromine from CFCs and halons led to a decrease of ozone in the simulations to a minimum near 2000, followed by an increase as the CFCs and halons are removed from the stratosphere. A decrease in the ozone concentration due to an increase in chlorine-catalyzed loss leads to a decrease in ozone heating and temperature. The ozone change and the temperature change are in the same direction. The decrease in temperature feeds back to modify the change in ozone through the temperature dependence of the photochemical reactions (see, e.g., Barnett et al. 1975; Douglass and Rood 1986 and references therein for more details on ozone–temperature relations in the upper stratosphere). This feedback reduces the impact of the increase in chlorine on ozone.

The annual-average temperature calculated in the 140-yr simulation using the GEOS CCM for the northern midlatitude upper stratosphere (40°N, 1 hPa) decreases over the entire time period of the simulation as shown in Fig. 1. The rate of decrease is largest in the years from about 1980 to 2000—the period of the largest ozone decrease. The results of the time series analysis, showing the fit to the entire record and the contributions of the individual terms, are shown in Fig. 1.

Table 1 gives the sensitivity coefficients a_1, a_2, and a_3 obtained by analyzing the entire time series at 40°N, 1 hPa as described above. The units of each coefficient are temperature change in kelvin per unit change of the mixing ratio of the constituent, expressed in the table as parts per billion by volume (ppbv) or parts per million by volume (ppmv). Thus the sensitivity to EESC at this location in the atmosphere for the simulation is -0.92 K ppbv^{-1} or about a 1-K decrease in temperature for each added ppbv of equivalent chlorine. The table also

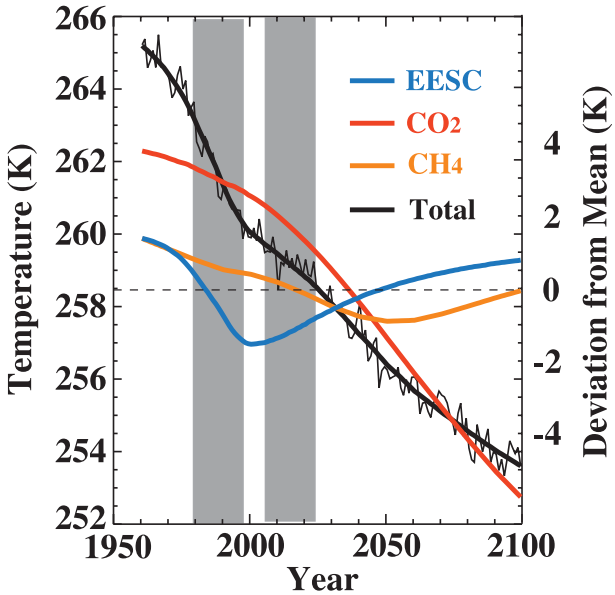

FIG. 1. Time series fit of simulated temperatures at 40°N, 1 hPa (thin black line) with the statistical fit shown as the heavy black line. Scale on left shows temperatures for the time series. Scale on the right shows deviations from the mean for the terms due to changes in EESC (blue line), CO_2 (red line), and CH_4 (orange line).

shows how this sensitivity affects temperature during two 20-yr time periods. Between 1979 and 1998 the EESC increased by 2.1 ppbv resulting in a temperature decrease of 1.9 K at 1 hPa, 40°N. For the second time period (2006–25) the EESC in the simulation decreased by 0.76 ppbv accompanied by a temperature increase of 0.7 K.

Although the sensitivity to CO_2 is -0.024 K ppmv^{-1}, the change in CO_2 over the 1979–98 time period is 29 ppmv, yielding a simulated temperature change at 1 hPa of -0.7 K. This decrease of 0.7 K due to CO_2 increase should be compared with the decrease of 1.9 K due to EESC. During the next two decades (2006–25) the CO_2 input to the simulation increased by 55 ppmv, yielding a temperature decrease of 1.3 K. The temperature decrease owing to the methane increase for 2006–25 (0.6 K) is also larger than for 1979–98 (0.4 K). Note that

TABLE 1. Summary of sensitivities at 40°N, 1 hPa. The sensitivity for a change of 1 ppbv or 1 ppmv is shown in the first column of numbers. The next column shows the change in the concentration of each species between 1979 and 1998. The third column shows the simulated temperature change from 1979 to 1998 that is attributed to each term. The fourth and fifth columns show the change in concentration and temperature for each term for 2006–25. Uncertainties are 2σ.

		1979–98		2006–25	
Term	a	ΔMR	ΔT (K)	ΔMR	ΔT (K)
EESC	-0.92 ± 0.1 K ppbv^{-1}	+2.1 ppbv	-1.9 ± 0.2	-0.76 ppbv	$+0.7 \pm 0.1$
CO_2	-0.024 ± 0.001 K ppmv^{-1}	+29 ppmv	-0.7 ± 0.03	+55 ppmv	-1.3 ± 0.05
CH_4	-2.0 ± 0.3 K ppmv^{-1}	+0.19 ppmv	-0.4 ± 0.06	+0.29 ppmv	-0.6 ± 0.09
Total			-3.0 ± 0.2		-1.2 ± 0.14

it is only possible to separate the CH_4 signal in the time series from the CO_2 signal when the time series extends beyond 2060. For a scenario in which CH_4 continues to increase it would not be possible to separate its signature from that of CO_2 by this technique.

Overall, the temperature in the midlatitude upper stratosphere changed by 3 K, or 1.5 K decade^{-1}, in our model simulations for the 20-yr period from 1979 to 1998. Nearly two thirds of the temperature change between 1979 and 1998 at 1 hPa is attributable to the increase in EESC and associated decrease in heating by O_3 absorption of ultraviolet radiation. For the next 20 years, continued increases in cooling due to greenhouse gas increases compete with increased heating by ultraviolet absorption as ozone increases in response to the EESC decrease. The net temperature decrease for 2006–25 is half that of 1979–98 even though both CO_2 and CH_4 grow more rapidly during this period (see also Eyring et al. 2007 and Shepherd and Jonsson 2008 for similar results from other models). The temperature increase due to the decrease in ozone-depleting substances does not overwhelm the continued greenhouse gas contribution because the rate of decrease of EESC is only about one-third its rate of increase during 1980s and 1990s.

b. *Midlatitude lower stratosphere: Latitude = 40°N, pressure = 50 hPa*

The midlatitude lower stratosphere of the Northern Hemisphere has long been a region of interest for possible temperature trends. At first, attention was directed toward the effects of increasing carbon dioxide. Epstein (1982) suggested that a way to detect the atmospheric impact of CO_2 would be in the expected opposite signatures: heating in the troposphere and cooling in the lower stratosphere. He suggested that it might be possible to observe the opposite trends by 1986. Angell (1986), using data from 1965 through 1985, reported cooling of the lower stratosphere and attributed the cooling to CO_2. Miller et al. (1992) analyzed radiosonde data and ozonesonde data and found negative trends in both temperature and ozone, suggesting that the temperature trends were caused by the ozone trends. Randel and Cobb (1994) pointed out the trends through 1992 deduced from the Microwave Sounding Unit (MSU) channel 4 data for winter–spring were consistent in space–time patterns with the deduced ozone trends for the Northern Hemisphere lower stratosphere. They concluded that ozone was the most important driver of the lower-stratospheric temperature trends. But, they also report a lack of temperature trends in Southern Hemisphere lower stratosphere despite large ozone losses. McCormack and Hood (1994) showed one-dimensional radiative–convective model calculations of temperature changes for specified ozone changes in the Northern Hemisphere that were consistent with the results of Randel and Cobb (1994).

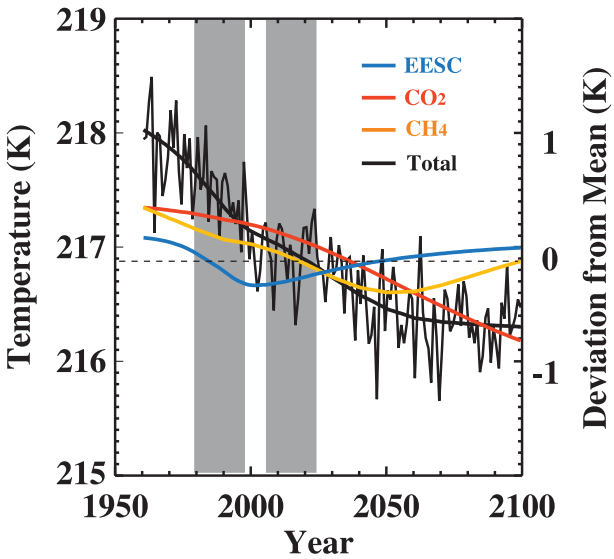

FIG. 2. As in Fig. 1 but at 40°N, 50 hPa.

Ramaswamy et al. (1996) put observed ozone changes into their general circulation model and confirmed that the temperature trends followed the fingerprint of the seasonal and latitudinal variation of the ozone trends. Langematz et al. (2003) also used a GCM forced with observed ozone change and with specified CO_2 change. Their simulations did not produce trends in the northern midlatitude lower stratosphere that were as large as those observed in the Free University of Berlin data, thus they concluded that the observed cooling could not be explained by the observed ozone and CO_2 changes. Shine et al. (2008) have revisited the temperature trends

TABLE 2. Summary of terms for 40°N, 50 hPa and changes for two time periods, columns as described for Table 1.

		1979–98		2006–25	
Term	a (K ppbv^{-1})	ΔMR	ΔT (K)	ΔMR	ΔT (K)
EESC	−0.13 ± 0.08 K ppbv^{-1}	+2.1 ppbv	−0.3 ± 0.2	−0.76 ppbv	+0.1 ± 0.06
CO_2	−0.0029 ± 0.0008 K ppmv^{-1}	+29 ppmv	−0.09 ± 0.03	+55 ppmv	−0.16 ± 0.05
CH_4	−0.66 ± 0.3 K ppmv^{-1}	+0.19 ppmv	−0.13 ± 0.06	+0.29 ppmv	−0.19 ± 0.09
Total			−0.5 ± 0.2		−0.25 ± 0.1

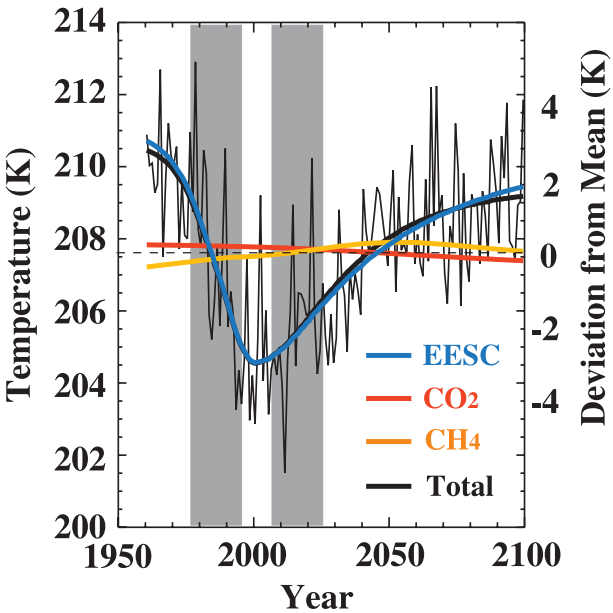

FIG. 3. As in Fig. 1 but at 88°S, 100 hPa.

derived from the Stratospheric Sounding Unit (SSU) satellite instruments (an infrared radiometer that measures upwelling radiation in the 15-μm band of CO_2). Application of a radiance correction for changing CO_2 with time resulted in adjustments to the deduced temperature trends that are closer to those derived by most models. Similarly, Free et al. (2005) reevaluated the sonde data and obtained temperature trends closer to model results. These are shown below in section 4.

Figure 2 shows the simulated temperature time series along with the regression components obtained from the time series analysis. Table 2 gives the sensitivities and also the changes for 1979–98 and 2006–25 determined by multiplying the sensitivities by the change in constituent concentration for each time period as was done in Table 1 above for 1 hPa.

The overall change for 1979–98 in the lower northern midlatitude stratosphere (at 40°N, 50 hPa) from our simulations is −0.5 K over two decades. Approximately 60% of the simulated trend during this time period came from the change in EESC. The change in temperature due to change in methane is greater than that due to change in CO_2. Note that the CH_4 term also includes any effect from the increase of water vapor from CH_4 oxidation. The fit gives a negative trend for the 2006–25 period. Examination of the time series over that short time period shows significant variability and a linear fit over those few years would give a near-zero, or possibly positive, trend that would not be significant. This points out the importance of long time series especially in regions such as the northern midlatitudes.

c. *Antarctic lower stratosphere: Latitude = 88°S, pressure = 100 hPa*

The temperature change in the lowermost Antarctic stratosphere is almost completely due to the ozone change generated by ozone-depleting substances in the Antarctic ozone hole over the entire time period. In this region the effects of CO_2 and other greenhouse gases are nearly zero. This is also the point of maximum ozone change in the Antarctic ozone hole, and feedbacks such as those operating in the upper stratosphere are not important.

Figure 3 shows the simulated temperature time series and the sensitivities to EESC, CO_2, and CH_4 at 88°S, 100 hPa. Table 3 shows these sensitivities and temperature changes for the two time periods. As expected, the EESC term is large and the temperature change due to change in EESC is by far the largest. Note that the decrease in EESC and the increase in temperature from 2006 to 2025 are only about one-third of the changes that occurred from 1979 to 1998.

d. *Antarctic upper stratosphere: Latitude = 88°S, pressure = 5 hPa*

Dynamic feedback in the Antarctic upper stratosphere causes a warming in response to the increased cooling in the Antarctic lower stratosphere due to the ozone hole (Kiehl et al. 1988; Mahlman et al. 1994). A change in the downward circulation and flux of ozone in this region has been shown to produce a summertime increase in ozone and in temperature in the middle stratosphere over the Antarctic (Stolarski et al. 2006a). The perturbation that produces the dynamic heating above the ozone hole decreases as ozone recovers. The temperature trend in this region is eventually dominated by cooling due to greenhouse gases (see Fig. 4 and Table 4).

TABLE 3. As in Table 2 but for 88°S, 100 hPa.

		1979–98		2006–25	
Term	a	ΔMR	ΔT (K)	ΔMR	ΔT (K)
EESC	-2.0 ± 0.2 K ppbv^{-1}	+2.1 ppbv	-4.0 ± 0.4	−0.76 ppbv	$+1.5 \pm 0.15$
CO_2	-0.002 ± 0.002 K ppmv^{-1}	+29 ppmv	-0.03 ± 0.03	+55 ppmv	-0.06 ± 0.06
CH_4	-0.85 ± 0.7 K ppmv^{-1}	+0.19 ppmv	-0.12 ± 0.1	+0.29 ppmv	-0.17 ± 0.15
Total			-4.1 ± 0.4		$+1.3 \pm 0.2$

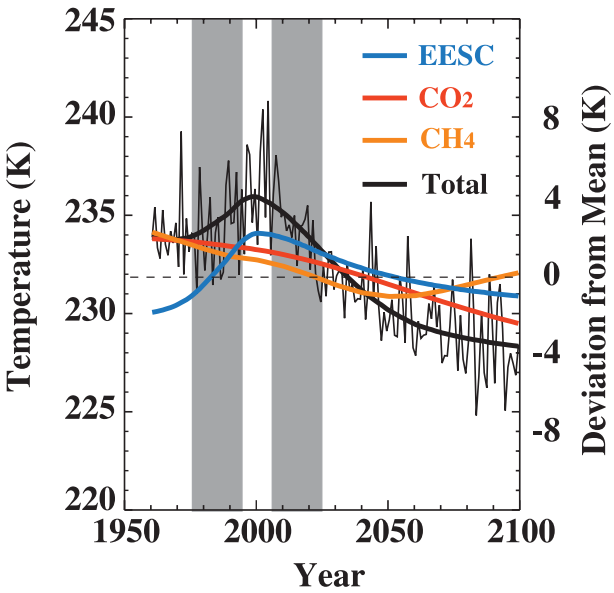

FIG. 4. As in Fig. 1 but at 88°S, 5 hPa.

e. *Summary of fits throughout the atmosphere*

We have demonstrated that we can analyze the individual time series at specific locations in the atmosphere from a 140-yr simulation to determine the relative sensitivities of EESC and greenhouse gases. These sensitivities were then converted to the implied contributions from the mixing ratio changes for EESC and greenhouse gases for two time periods: the historical record from 1979 through 1998 and the near future from 2006 through 2025. We emphasize that these results are based on our model simulations. Analysis of real data will not have the advantage of the 140-yr time series that we used to develop these results.

The simulated annual-average temperature changes in kelvin for 1979–98 are shown as a function of latitude and pressure altitude in Fig. 5. These changes are derived from the fitting parameters described in the previous section. The general result is a cooling of the stratosphere with a warming of the troposphere. The ozone hole cooling in the lower Antarctic stratosphere and the indirect dynamical warming above it (e.g., Mahlman et al. 1994) are clearly shown. The top-left panel of Fig. 5 shows the total change; the middle-left panel shows the contribution due to EESC (or ODSs); the bottom-left panel shows the contribution due to GHGs.

The right panels of Fig. 5 show the total 2006–25 temperature change, the ODS contribution, and the GHG contribution. The reversal of ozone loss switches the sign of the Antarctic lower-stratospheric cooling and upper-stratospheric warming. The crossover between tropospheric warming and stratospheric cooling occurs well above the tropopause in the middle and high latitudes of both hemispheres. Warming extends up to 35 hPa in the Antarctic and 60 hPa in the Arctic. This 2006–25 warming also extends downward into the troposphere over Antarctica. The amount of cooling in the tropical and midlatitude upper stratosphere is decreased because of the simulated ozone increase in this region.

For the time period from 1979 to 1998, both ODSs and GHGs led to a cooling. Figure 6 shows the relative contribution of both of these sources of cooling for this time period. The contribution to cooling from ODSs reaches a maximum of greater than 70% between 1 and 3 hPa over a broad range of latitudes. The ODS contribution is minimum in the middle stratosphere reaching lower than 10% at high northern latitudes. In the lower stratosphere, the contribution of cooling due to ODSs again becomes large as the GHG term approaches zero. In the lowermost stratosphere, the GHG term becomes positive, indicating warming. This region is left blank in Fig. 6 as the two terms have opposite signs and the ratio has no meaning. These numbers are based on our assumption of linearity in the response of temperature to CO_2 increases. It has been pointed out to us (A. Jonsson 2008, personal communication; Jonsson et al. 2009) that the response may not be linear. We tested our results and found that an assumed nonlinearity similar to that suggested by Jonsson et al. (2009) would reduce the 70% maximum to about 63%.

4. Comparison of simulated trends to those from data and other models

Shine et al. (2003) have compared a number of chemistry–climate model simulations of past temperature change with data. Figure 7 compares our results for

TABLE 4. As in Table 2 but for 88°S, 5 hPa.

		1979–98		2006–25	
Term	a	ΔMR	ΔT (K)	ΔMR	ΔT (K)
EESC	$+1.3 \pm 0.2$ K ppbv^{-1}	+2.1 ppbv	$+2.6 \pm 0.4$	−0.76 ppbv	-1.0 ± 0.2
CO_2	-0.011 ± 0.002 K ppmv^{-1}	+29 ppmv	-0.3 ± 0.06	+55 ppmv	-0.6 ± 0.1
CH_4	-2.9 ± 0.8 K ppmv^{-1}	+0.19 ppmv	-0.6 ± 0.2	+0.29 ppmv	-0.8 ± 0.2
Total			$+1.7 \pm 0.5$		-2.4 ± 0.4

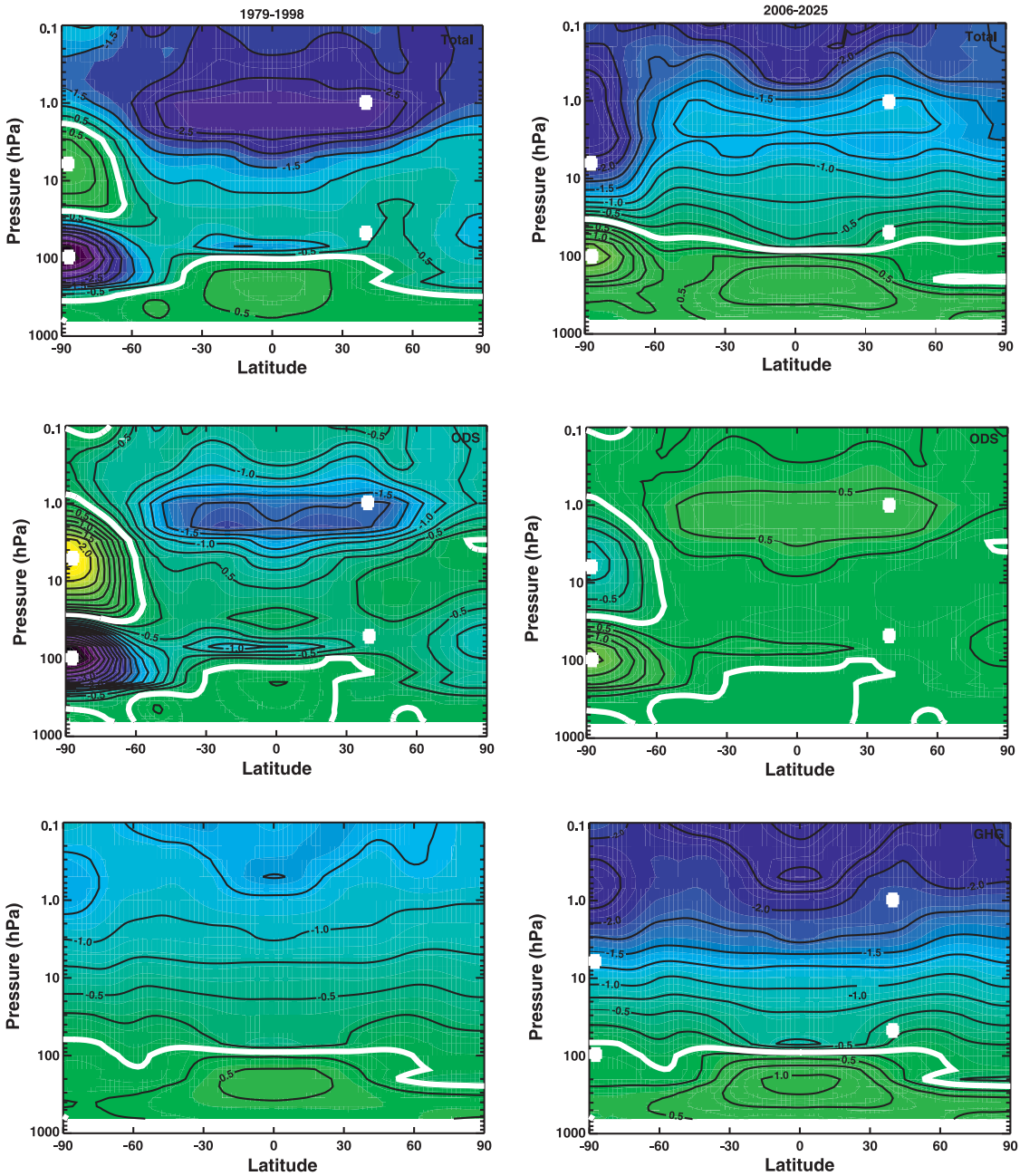

FIG. 5. (left) Temperature change (K) (left) from 1979 to 1998 and (right) from 2006 to 2025 for GEOS CCM simulations: (top) total temperature change, (middle) change due to ozone-depleting substances, and (bottom) change due to greenhouse gases. Dividing by 2 will give the temperature trends in K decade^{-1} for each of the 20-yr time periods. White plusses indicate the locations analyzed in Figs. 1–4.

the global mean temperature trend between 1979 and 1998 with the range of models from Shine et al. (2003) and with the Canadian Middle Atmosphere Mode (CMAM) model as reported by Shepherd and Jonsson (2008). Figure 7 also compares our results with trends derived from the combined MSU and SSU satellite instruments (updated by Shine et al. 2008) and with trends derived from radiosondes (Lanzante et al. 2003a,b; updated by Free et al. 2005 and Lanzante 2007). With the updates in the temperature time series and trends, the trends derived from our simulations agree reasonably well with those derived from data. Note that Pawson et al. (2008) found that the GEOS CCM shows stratospheric temperature changes that are within the range of

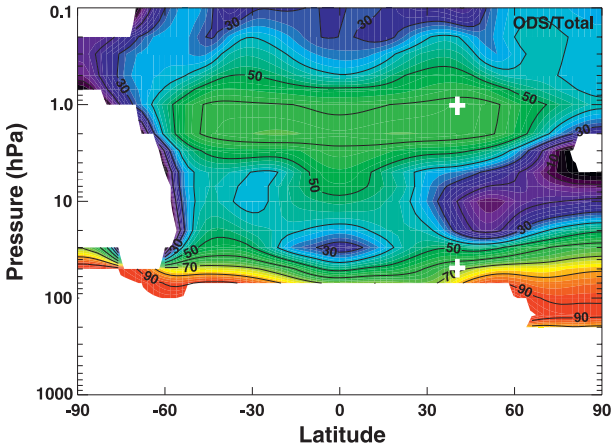

FIG. 6. Ratio of temperature decrease (%) due to ODS to the total temperature decrease from 1979 through 1998. Results shown only where both ODS and GHG are calculated to be causing a negative temperature trend. Plusses indicate the locations analyzed in Figs. 1–4.

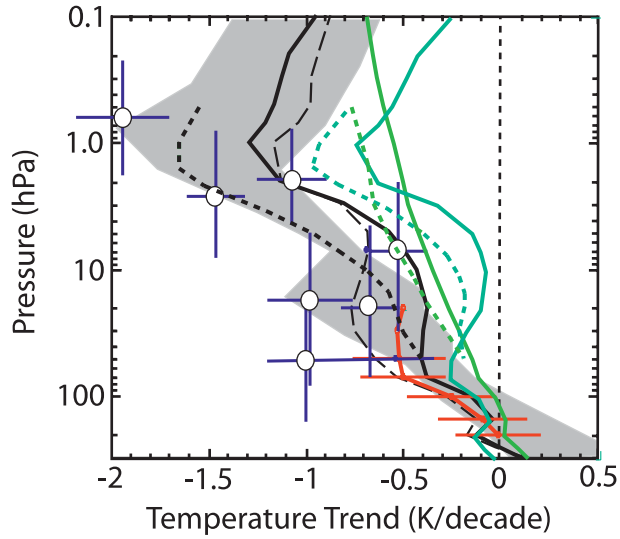

FIG. 7. Comparison of simulated global temperature trend for 1979–99 with trends derived from data. Solid black line is the mean trend for the time period derived from the sensitivity coefficients obtained by statistical analysis of the entire 1960–2100 time series. The dashed line is the linear trend calculated from the 1979–99 period of the simulation. The solid green line shows the contribution of GHG to the trend according to Shine et al. (2003) while the dashed green line shows the contribution of GHG to the trend from the CMAM model according to Jonsson et al. (2009). The light blue line shows the contribution of ozone change from Shine et al. (2003) while the dashed blue line shows the ODS term from CMAM. The short-dashed black line is the total cooling from CMAM. Blue crosses indicate satellite temperature trends derived from SSU and MSU as revised by Shine et al. (2008). Red line and crosses indicate sonde temperature trends [Radiosonde Atmospheric Temperature Products for Assessing Climate (RATPAC)] as derived by Free et al. (2005). Shaded area indicates range of models shown by Shine et al. (2003).

those computed using other models but that the cooling was at the weaker end of the range found in prior publications. Two results from the simulations are shown in Fig. 7. One (solid black line) is calculated from the sensitivities from the analysis described above while the other (dashed black line) is a trend calculated for 1979–98 using the same approach as used to derive the trends from observations, that is, a simple linear trend.

We have used the time signatures in our simulations to separate the contributions of the changes in EESC from the contributions of the greenhouse gases CO_2 and CH_4 to temperature change. Figures 1–4 interpret this separation at four specific locations. Figure 7 shows the results as a function of altitude averaged over most of the globe (60°S–60°N). The range from simulations by other models, as summarized by Shine et al. (2003), is also shown in Fig. 7. Note that our results agree well in shape with those from the CMAM simulations reported in Shepherd and Jonsson (2008) as updated by Jonsson et al. (2009), but we obtain a smaller cooling throughout the stratosphere. In the next section we consider how long a dataset would have to be to begin to achieve a statistically significant separation of the changes due to EESC and GHG.

5. Detection in data: How long does it take?

We have shown that we can separate the contributions to change in the 140-yr simulated time series using statistical analysis. Here we consider how many years of output from the simulation are required before the analysis can separate the terms with statistical significance. The number of years required depends on location. At some locations the temperature trends are not significant even when the entire simulation time series is used. Clearly it will not be possible to identify separate contributions to trends in these regions by time series analysis. Other regions have significant trends, and it is possible to separate the causes of the trends in the simulated time series. We attempt to determine the minimum length of record to separate the terms in the regions where we have derived statistically significant trends.

We repeat the analysis of previous sections with 1979 as the starting point and a variable end point. For this part of the study we examined ending points ranging from 2000 to 2050. During this period the CO_2 and CH_4 terms are not distinct and the terms cannot be separated. We thus apply a statistical model that includes only the EESC and CO_2 terms. The results are expressed as sensitivity coefficients for either EESC or CO_2 (see Tables 1–4).

Figure 8 illustrates sensitivity of the statistical analysis to the length of record for a single point in the atmosphere (40°N, 1 hPa). When the time series is short, the addition

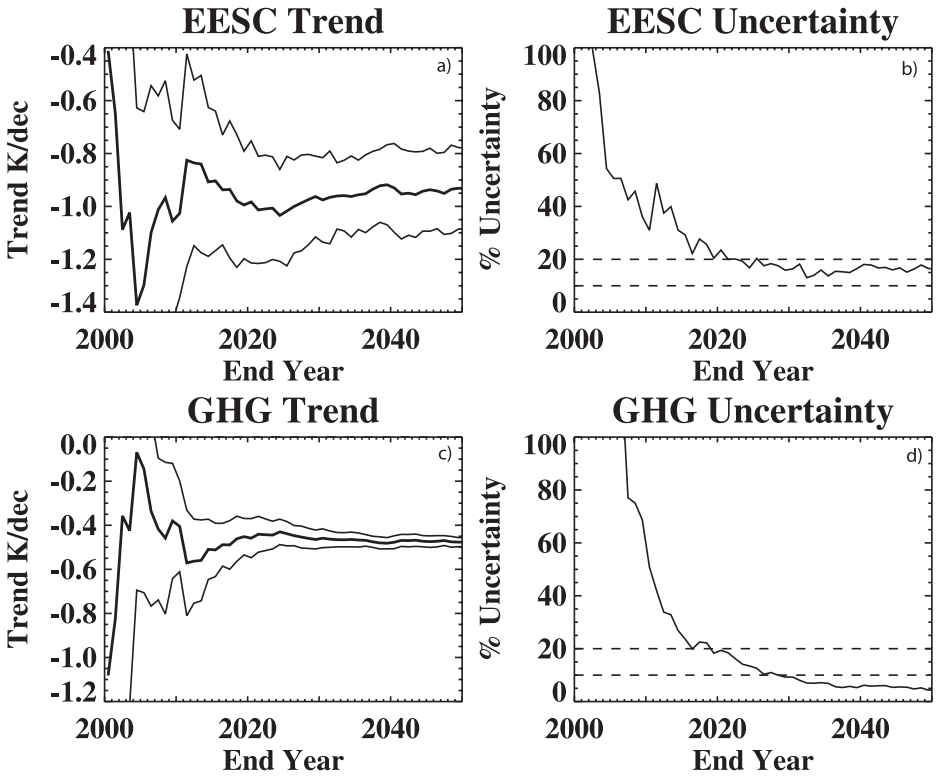

FIG. 8. (a) Sensitivity of temperature (for the time period 1979–98) at 40°N, 1-hPa pressure altitude to EESC from analysis of the time series. Heavy line is the sensitivity (a_1) calculated as a function of the endpoint of the time series. The thin lines are the 2σ uncertainty limits. (b) Absolute value of 2σ uncertainty for the EESC term. Dashed lines show 20% and 10% levels. (c) Same as (a) for the greenhouse gas (CO_2) sensitivity. (d) Same as (b) for the greenhouse gas uncertainty.

of a few years of data can change the answer by a large amount. As the time series lengthens, the derived trend becomes insensitive to the endpoint. We can see in Fig. 8 that the deduced sensitivity to EESC fluctuates between -0.5 and -1.4 K ppbv^{-1} as the endpoint of the time series is extended from 2000 to 2010. The term is significantly different from zero for all endpoints past 2003. By about 2020, the EESC term is known to within 20% uncertainty. The CO_2 term fluctuates between -0.01 and -0.1 K ppmv^{-1} for endpoints between 2000 and about 2010. By about 2020 the CO_2 term stabilizes at about -0.05 K ppmv^{-1} with an uncertainty of less than 10%.

Figure 9 shows similar results for the lower midlatitude stratosphere. Here we see that the deduced sensitivity to EESC changes sign as the time series lengthens. Sensitivity to EESC is significantly different from zero when the time series extends to the year 2020, but uncertainty in the magnitude of this term is always 50% or greater. The sensitivity to CO_2 and its uncertainty also change rapidly as the length of time series is increased. Once the time series extends beyond about 2012, this term is significantly different from zero. By 2050, the deduced uncertainty in this term is about 20%.

6. Discussion and conclusions

We have analyzed composite time series of temperatures calculated using GEOS CCM for the 140-yr period 1960 through 2100. We use time series analysis to separate contributions to temperature change due to EESC-induced ozone change from those due to increasing greenhouse gases. In the long-term (through 2100) the greenhouse gas contributions to temperature change dominate. The stratosphere cools and the troposphere warms.

Several factors contributed to the annually averaged temperature change in the stratosphere between 1979 and 1998. The most important of these were ozone, carbon dioxide, and methane. In our simulation, EESC-induced ozone change accounted for about 70% of the temperature change in the upper stratosphere (1–3 hPa) for this time period. We also find that this ozone change accounted for less than about 30% of the temperature change in the middle stratosphere and most of the temperature change in the lowermost stratosphere. This is consistent with the conclusion drawn by Shine et al. (2003) from data and model sensitivity calculations.

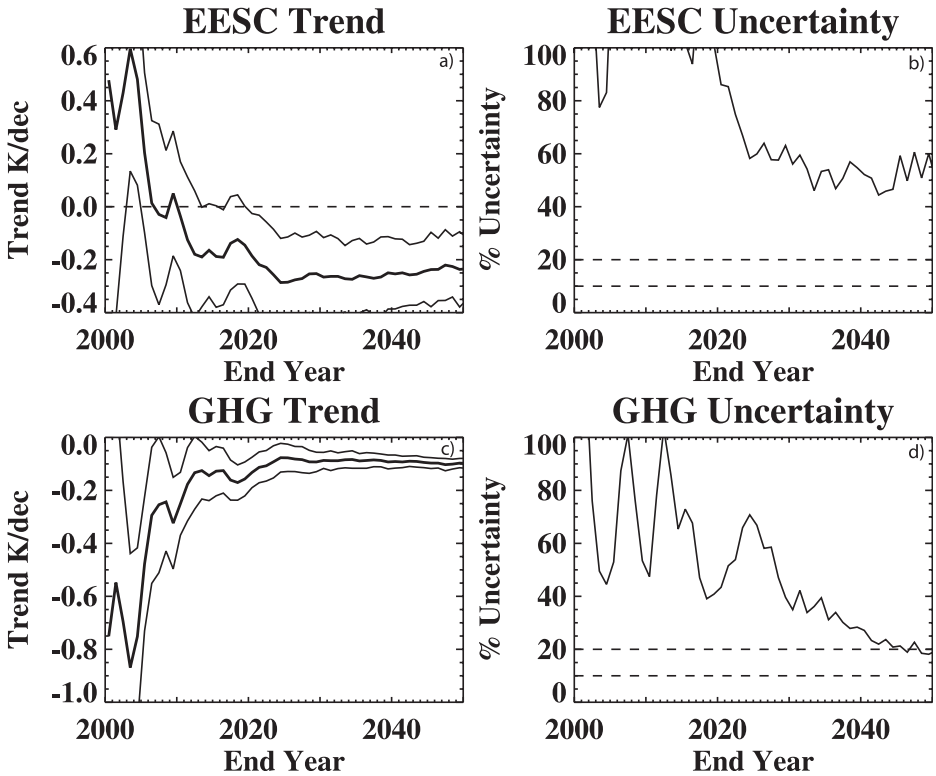

FIG. 9. As in Fig. 7 but for 40°N, 50-hPa.

In the Antarctic lower stratosphere, the temperature change is dominated by the EESC-induced ozone change throughout the 140 years of simulation with very small contributions from GHGs.

Analysis of our simulations indicates that during the next 20 years the ozone increase as EESC decreases and continued greenhouse gas increases will act in opposite directions in the stratosphere as previously pointed out by Eyring et al. (2007) and Shepherd and Jonsson (2008). Ozone recovery will lead to increased heating and a temperature increase, whereas greenhouse gases increases will lead to increased cooling and a temperature decrease. The increased heating from ozone recovery does not overwhelm the continued cooling from GHGs, partly because the rate of increase of ozone is only one-third of the rate of increase during the 1980s and 1990s. In the midlatitude upper stratosphere these combine to slow the rate of temperature decrease over the next 20 years. The same is true of the midlatitude lower stratosphere where we expect the temperature decrease over the next two decades to be only half of what it has been over the last two decades. In the Antarctic lower stratosphere, the temperature should increase over the next 20 years as the ozone hole recovers. All results for the future are for a specific scenario (Ab scenario for ODSs and A1 scenario for GHGs). Most of the conclusions stated above would hold for other proposed scenarios, although the numerical details would be a little different.

The one exceptional region is the Antarctic upper stratosphere near 5 hPa where temperature in the simulations increased over the last two decades (Stolarski et al. 2006a). This increase is expected to switch to a decrease over the next two decades and beyond as the ozone hole and the subsequent seasonally dependent dynamical response to it diminish.

Using output from our simulations we determined that significant separation of the ozone-depleting substance (EESC) from greenhouse gas (CO_2) impacts on temperatures in the upper stratosphere could be achieved using output from 1979 through about 2010. The Antarctic and midlatitude lower stratosphere require longer time series. The application of these results to real atmospheric data depends on the realism of the model-calculated sensitivities and the realism of model variability. Other factors such as solar cycle variability must be included in the time series analysis of observations.

Acknowledgments. Thanks to NASA for high-performance computing resources on ''Project Columbia'' and staff at NAS for assistance in keeping the models running. We thank NASA's MAP Program for funding.

TABLE A1. Simulations of GEOS CCM used in this study. Start year is the beginning of the simulation. Analysis start is the first year used to construct the time series, discarding spinup years.

Simulation	SSTs	Start (yr)	Analysis start	End (yr)
P1	Observed	1950	1960	2004
P2	Observed	1950	1960	2004
F1	HadGEM1	1996	2005	2099
F2	HadGEM1	1971	1980	2052
F3	NCAR CCSM3	1971	1980	2050
F4	NCAR CCSM3	2000	2005	2099

APPENDIX

Construction of Time Series from Model Simulations

The results in this paper have been based on one simulated time series constructed from two separate simulations: the past from 1960 to 2004 and the future from 2004 to 2099 (labeled P1 + F1). In this appendix, we describe six simulations (see Table A1) that were used to construct four time series of temperatures at each model grid point for the time period from 1960 through 2099. These time series are not independent, as they use only two past simulations for the period 1960–2004.

A problem in constructing these time series is that the SSTs from each of the three sources (observed, HadGEM1, and CCSM3) are not consistent with one another. The tropical SSTs in the HadGEM1 are 1–2 K colder than in the observations and CCSM3. This and other differences lead to a bias in atmospheric temperatures.

The main problem for constructing the 140-yr time series that we need for analyses is the difference between the observed SSTs, the HadGEM1 SSTs, and the CCSM3 SSTs each of the model-generated SSTs. The difference between the stratospheric temperatures for simulations using HadGEM1 and CCSM3 SSTs is shown in Figure A1. The difference shown is the average over 69 years of overlap of the simulations F2 and F3 between the years 1980 and 2049. The cooler tropical SSTs in HadGEM1 lead to a cooler tropical troposphere and a warmer region just above the tropical tropopause. The colder sea surface temperatures in simulations with HadGEM1 create a weaker tropical upwelling. The tropical lower stratosphere is a region in which ozone production is occurring in ozone-poor air upwelling from the troposphere. Ozone concentration is determined by ozone production balanced by upwelling of ozone-poor air. If the rate of upwelling is reduced, then more ozone can be produced, resulting in warmer temperatures. Weaker upwelling also produces a weaker overturning circulation throughout the stratosphere. The result is less downwelling in the extratropics and colder temperatures there because the weaker downwelling effectively heats the atmosphere.

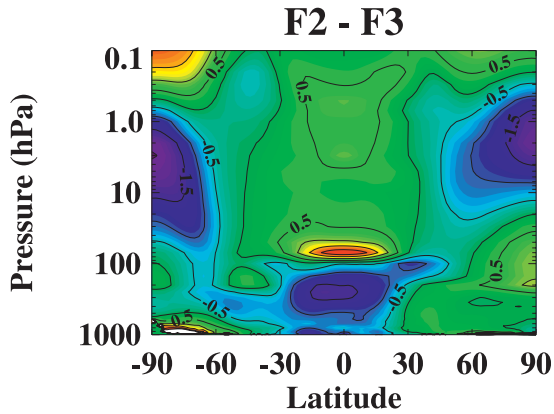

FIG. A1. Annual-average temperature difference between F2 simulation using HadGEM1 SSTs and F3 simulation using CCSM3 SSTs. Average uses overlap period from 1980 to 2049.

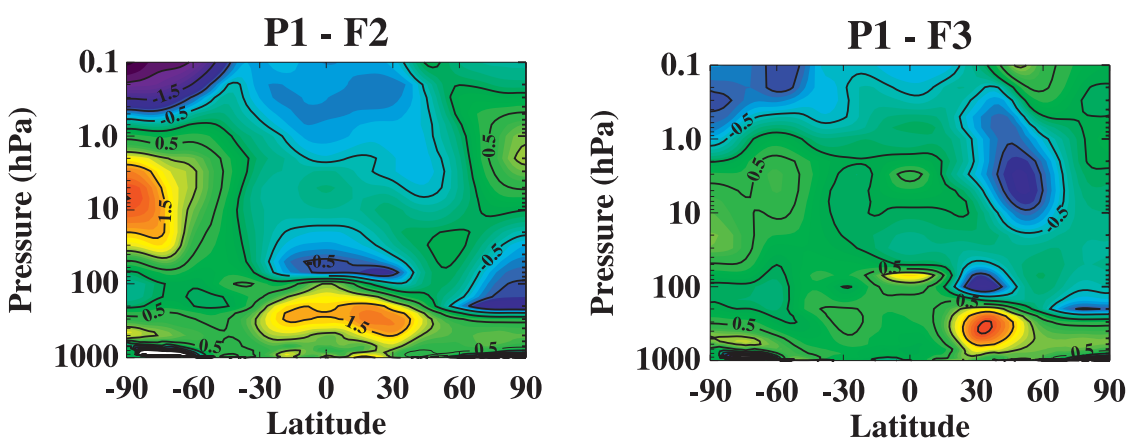

FIG. A2. Annual-average temperature difference between the past simulation, P1, using observed SSTs and the future simulations, F2 and F3, using HadGEM1 and CCSM3 SSTs, respectively. Average is for overlap between 1980 and 2004.

TABLE A2. Simulations used to construct the 1960–2100 time series. Middle column indicates simulations used. Right column indicates simulations used to determine adjustment factors for consistency of overall time series.

Series	Simulations	Overlap adjustment
A	P1 (1960–2004)/F1 (2005–99)	P1/F2 (1980–2004)
B	P2 (1960–2004)/F1 (2005–99)	P2/F2 (1980–2004)
C	P1 (1960–2004)/F4 (2005–99)	P1/F3 (1980–2004)
D	P2 (1960–2004)/F4 (2005–99)	P2/F3 (1980–2004)

Figure A2 shows the bias between the P1 simulation using observed SSTs and each of the F2 and F3 simulations. The differences between P1 and F2 (HadGEM1 SSTs) are significantly greater than those between P1 and F3 (CCSM3 SSTs). The differences between P2 and F2 or F3 are similar to those between P1 and F2 or F3 and are not shown. The differences between simulations using the same SSTs are small (e.g., P1 and P2; F1 and F2; F3 and F4). The differences shown in Figure A2 were averaged over 25 years of simulation and have been used as additive adjustments (constant in time) to put the past and future simulations together to form continuous time series for the analysis in the rest of this paper.

Table A2 lists the four time series that were constructed from these simulations after allowing for adjustments. The result of the process described above is four time series that extend from 1960 through the end of 2099. These are not completely independent time series as only two past and two future simulations were used, but they will give some indication of the variability that will occur between ensemble members of the simulations by the GEOS CCM.

Figure A3 shows time series for four locations in the stratosphere that were featured in section 3 of this paper. These are the northern midlatitude upper stratosphere (40°N, 1 Pa), the northern midlatitude lower stratosphere (40°N, 50 hPa), the south polar lower stratosphere (88°S, 100 hPa), and the south polar upper stratosphere (88°S, 5 hPa).

These four locations were chosen in section 3 to illustrate different aspects of the interaction between forcing due to greenhouse gases and forcing due to ozone change. Figure A3 illustrates that the main features discussed are present in all of the time series constructed from our GEOS CCM simulations. In the northern midlatitude upper stratosphere, the temperature decreases over the entire simulation with a clear acceleration during the

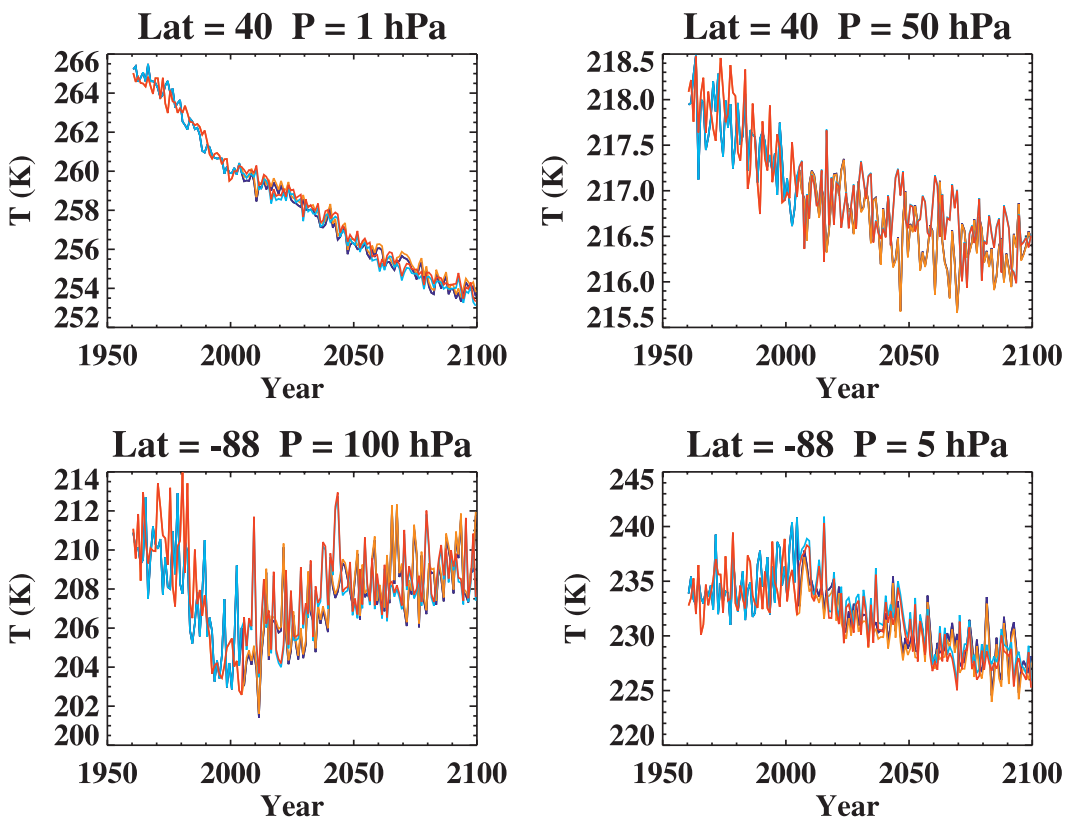

FIG. A3. Time series at four locations: light and dark blue curves (orange and red curves) have P1 simulation (P2 simulation) in common.

TABLE A3. Summary of sensitivity coefficients at 1 hPa, 40°N latitude for EESC, CO_2, and CH_4 for each of the four time series showing variability among ensemble members of the same basic simulation. Uncertainties are 2σ.

Term	P1F1	P2F1	P1F4	P2F4
EESC (K $ppbv^{-1}$)	-0.92 ± 0.1	-0.82 ± 0.11	-0.91 ± 0.08	-0.81 ± 0.1
CO_2 (K $ppmv^{-1}$)	-0.024 ± 0.001	-0.023 ± 0.001	-0.025 ± 0.001	-0.024 ± 0.001
CH_4 (K $ppbv^{-1}$)	-2.0 ± 0.3	-1.9 ± 0.4	-2.0 ± 0.3	-1.8 ± 0.3

ozone-depletion time period of the last two decades. The northern midlatitude lower stratosphere also shows a decrease over the entire simulation with significantly more interannual variability and a possible acceleration of the trend due to ozone. The Antarctic lower stratosphere shows a strong decrease to about 2000 followed by an increase thereafter; a shape that looks much like what we expect from ozone control of the temperature change. The Antarctic upper stratosphere shows a temperature increase over the last few decades followed by a decrease over the rest of the simulation.

Table A3 shows the sensitivity coefficients obtained at 1 hPa, 40°N latitude from each of the four time series described above using the entire 140-yr time period of the simulation. The coefficients vary but they remain well within the uncertainties calculated by a bootstrap procedure applied to the residuals from the fit to the various time series. The conclusions reached in the main body of this paper are not dependent on which of the time series we use.

REFERENCES

Angell, J., 1986: Annual and global seasonal temperature changes in the troposphere and low stratosphere, 1960–85. *Mon. Wea. Rev.,* **114,** 1922–1930.

Baldwin, M., and Coauthors, 2007: Climate–ozone connections. *Scientific Assessment of Ozone Depletion: 2006,* World Meteorological Organization Global Ozone Research and Monitoring Project, Rep. 50, World Meteorological Organization, 5.1–5.49.

Barnett, J. J., J. T. Houghton, and J. A. Pyle, 1975: The temperature dependence of the ozone concentration near the stratopause. *Quart. J. Roy. Meteor. Soc.,* **101,** 245–257.

Blake, D., and R. S. Lindzen, 1973: Effect of photochemical models on calculated equilibria and cooling rates in the stratosphere. *Mon. Wea. Rev.,* **101,** 783–802.

Collins, W. D., and Coauthors, 2006: The Community Climate System Model Version 3 (CCSM3). *J. Climate,* **19,** 2122–2143.

Douglass, A. R., and R. B. Rood, 1986: Derivation of photochemical information near 1-mbar from ozone and temperature data. *J. Geophys. Res.,* **91,** 3153–3166.

——, and S. R. Kawa, 1999: Contrast between 1992 and 1997 high-latitude spring Halogen Occultation Experiment observations of lower stratospheric HCl. *J. Geophys. Res.,* **104,** 18 739–18 754.

——, C. H. Jackman, and R. S. Stolarski, 1989: Comparison of model results transporting the odd nitrogen family with results transporting separate odd nitrogen species. *J. Geophys. Res.,* **94** (D7), 9862–9872.

——, R. S. Stolarski, M. R. Schoeberl, C. H. Jackman, M. L. Gupta, P. A. Newman, J. E. Nielsen, and E. L. Fleming, 2008: Relationship of loss, mean age of air and the distribution of CFCs to stratospheric circulation and implications for atmospheric lifetimes. *J. Geophys. Res.,* **113,** D14309, doi:10.1029/2007JD009575.

Epstein, E. S., 1982: Detecting climate change. *J. Appl. Meteor.,* **21,** 1172–1182.

Eyring, V., and Coauthors, 2006: Assessment of temperature, trace species, and ozone in chemistry-climate model simulations of the recent past. *J. Geophys. Res.,* **111,** D22308, doi:10.1029/2006JD007327.

——, and Coauthors, 2007: Multimodel projections of stratospheric ozone in the 21st century. *J. Geophys. Res.,* **112,** D16303, doi:10.1029/2006JD008332.

Free, M., D. J. Seidel, J. K. Angell, J. Lanzante, I. Durre, and T. C. Peterson, 2005: Radiosonde Atmospheric Temperature Products for Assessing Climate (RATPAC): A new data set of large-area anomaly time series. *J. Geophys. Res.,* **110,** D22101, doi:10.1029/2005JD006169.

Haigh, J. D., and J. A. Pyle, 1979: A two-dimensional calculation including atmospheric carbon dioxide and stratospheric ozone. *Nature,* **279,** 222–224.

——, and ——, 1982: Ozone perturbation experiments in a two-dimensional circulation model. *Quart. J. Roy. Meteor. Soc.,* **108,** 551–574.

Johns, T. C., and Coauthors, 2006: The new Hadley Centre Climate Model (HadGEM1): Evaluation of coupled simulations. *J. Climate,* **19,** 1327–1353.

Jonsson, A. I., V. I. Fomichev, and T. G. Shepherd, 2009: An updated analysis of the attribution of stratospheric ozone and temperature changes to changes in ozone-depleting substances and well-mixed greenhouse gases. *Atmos. Chem. Phys. Discuss.,* **9,** 14 857–14 872.

Kiehl, J. T., B. A. Boville, and B. P. Briegleb, 1988: Response of a general circulation model to a prescribed Antarctic ozone hole. *Nature,* **332,** 501–504.

——, J. J. Hack, G. B. Bonan, B. A. Boville, D. L. Williamson, and P. J. Rasch, 1998: The National Center for Atmospheric Research Community Climate Model: CCM3. *J. Climate,* **11,** 1131–1149.

Langematz, U., M. Kunze, K. Kruger, K. Labitzke, and G. L. Roff, 2003: Thermal and dynamical changes of the stratosphere since 1979 and their link to ozone and CO_2 changes. *J. Geophys. Res.,* **108,** 4027, doi:10.1029/2002JD002069.

Lanzante, J. R., 2007: Diagnosis of radiosonde vertical temperature trend profiles: Comparing the influence of data homogenization versus model forcings. *J. Climate,* **20,** 5356–5364.

——, S. A. Klein, and D. J. Seidel, 2003a: Temporal homogenization of monthly radiosonde temperature data. Part I: Methodology. *J. Climate,* **16,** 224–240.

——, ——, and ——, 2003b: Temporal homogenization of monthly radiosonde temperature data. Part II: Trends, sensitivities, and MSU comparisons. *J. Climate,* **16,** 241–262.

Li, F., R. S. Stolarski, and P. A. Newman, 2009: Stratospheric ozone in the post-CFC era. *Atmos. Chem. Phys.,* **9,** 2207–2213.

Mahlman, J. D., J. P. Pinto, and L. J. Umscheid, 1994: Transport, radiative, and dynamical effects of the Antarctic ozone hole: A GFDL "SYYHI" model experiment. *J. Atmos. Sci.,* **51,** 489–508.

McCormack, J. P., and L. L. Hood, 1994: Relationship between ozone and temperature trends in the lower stratosphere: Latitude and seasonal dependences. *Geophys. Res. Lett.,* **21** (15), 1615–1618.

Miller, A. J., R. M. Nagatani, G. C. Tiao, X. F. Niu, G. C. Reinsel, D. Wuebbles, and K. Grant, 1992: Comparisons of observed ozone and temperature trends in the lower stratosphere. *Geophys. Res. Lett.,* **19,** 929–932.

Nakicenovic, N. and S. Swart, Eds., 2000: *Special Report on Emissions Scenarios*. Cambridge University Press, 599 pp.

Newman, P. A., J. S. Daniel, D. W. Waugh, and E. R. Nash, 2007: A new formulation of equivalent effective stratospheric chlorine (EESC). *Atmos. Chem. Phys.,* **7,** 4537–4552.

Oman, L., D. W. Waugh, S. Pawson, R. S. Stolarski, and J. E. Nielsen, 2008: Understanding the changes of stratospheric water vapor in coupled Chemistry–Climate Model simulations. *J. Atmos. Sci.,* **65,** 3278–3291.

Pawson, S., R. S. Stolarski, A. R. Douglass, P. A. Newman, J. E. Nielsen, S. M. Frith, and M. L. Guptha, 2008: Goddard Earth Observing System Chemistry Climate Model simulations of stratospheric ozone temperature coupling between 1950 and 2005. *J.Geophys. Res.,* **113,** D12103, doi:10.1029/2007JD009511.

Ramaswamy, V., M. D. Schwarzkopf, and W. J. Randel, 1996: Fingerprint of ozone depletion in the spatial and temporal pattern of recent lower-stratospheric cooling. *Nature,* **382,** 616–618.

Randel, W. J., and J. B. Cobb, 1994: Coherent variations of monthly mean total ozone and lower stratospheric temperature. *J. Geophys. Res.,* **99** (D3), 5443–5447.

Rayner, N. A., D. E. Parker, E. B. Horton, C. K. Folland, L. V. Alexander, D. P. Rowell, E. C. Kent, and A. Kaplan, 2003: Global analyses of sea surface temperature, sea ice, and night marine air temperature since the late nineteenth century. *J. Geophys. Res.,* **108,** 4407, doi:10.1029/2002JD002670.

Rosenfield, J. E., A. R. Douglass, and D. B. Considine, 2002: The impact of increasing carbon dioxide on ozone recovery. *J. Geophys. Res.,* **107,** 4049, doi:10.1029/2001JD000824.

Santer, B. D., and Coauthors, 2003: Contributions of anthropogenic and natural forcing to recent tropopause height changes. *Science,* **301,** 479–483.

Schauffler, S. M., and Coauthors, 2003: Chlorine budget and partitioning during the Stratospheric Aerosol and Gas Experiment (SAGE) III Ozone Loss and Validation Experiment (SOLVE). *J. Geophys. Res.,* **108,** 4173, doi:10.1029/2001JD002040.

Shepherd, T. G., and A. I. Jonsson, 2008: On the attribution of stratospheric ozone and temperature changes to changes in ozone-depleting substances and well-mixed greenhouse gases. *Atmos. Chem. Phys.,* **8,** 1435–1444.

Shine, K. P., and Coauthors, 2003: A comparison of model-simulated trends in stratospheric temperatures. *Quart. J. Roy. Meteor. Soc.,* **129,** 1565–1588.

——, J. J. Barnett, and W. J. Randel, 2008: Temperature trends derived from stratospheric sounding unit radiances: The effect of increasing CO_2 on the weighting function. *Geophys. Res. Lett.,* **35,** L02710, doi:10.1029/2007GL032218.

Stolarski, R. S., A. R. Douglass, M. Gupta, P. A. Newman, S. Pawson, M. R. Schoeberl, and J. E. Nielsen, 2006a: An ozone increase in the Antarctic summer stratosphere: A dynamical response to the ozone hole. *Geophys. Res. Lett.,* **33,** L21805, doi:10.1029/2006GL026820.

——, ——, S. Steenrod, and S. Pawson, 2006b: Trends in stratospheric ozone: Lessons learned from a 3D chemical transport model. *J. Atmos. Sci.,* **63,** 1028–1041.

Waugh, D. W., and V. Eyring, 2008: Quantitative performance metrics for stratospheric-resolving chemistry-climate models. *Atmos. Chem. Phys.,* **8,** 5699–5713.

WMO, 2003: *Scientific Assessment of Ozone Depletion: 2002*. Global Ozone Research and Monitoring Project, Rep. 47, World Meteorological Organization, 498 pp.